

MSP-FORMER: MULTI-SCALE PROJECTION TRANSFORMER FOR SINGLE IMAGE DESNOWING

Sixiang Chen^{1†}, Tian Ye^{1†}, Yun Liu^{2†}, Taodong Liao¹, Jingxia Jiang¹, Erkang Chen^{1,3}, Peng Chen^{1,3*}.

ABSTRACT

Snow removal causes challenges due to its characteristic of complex degradations. To this end, targeted treatment of multi-scale degradations is critical for the network to learn effective snow removal. In order to handle the diverse scenes, we propose a multi-scale projection transformer (MSP-Former), which understands and covers a variety of snow degradation features in a multi-path manner, and integrates comprehensive scene context information for clean reconstruction via self-attention operation. For the local details of various snow degradations, the local capture module is introduced in parallel to assist in the rebuilding of a clean image. Such design achieves the SOTA performance on three desnowing benchmark datasets while costing the low parameters and computational complexity, providing a guarantee of practicality.

1. INTRODUCTION

With the development of deep learning, low-level vision tasks have made great progress [1–5]. Snow removal from a single image is a complicated vision task because multiple ill-conditioned degradations (e.g. veiling effect, background occlusion, snow particles etc.) are superimposed on a snowy image. The imaging model of the snow scene can be modeled as:

$$I(x) = K(x)T(x) + A(x)(1 - T(x)), \quad (1)$$

where $I(x)$ represents the snowy image, $K(x) = J(x)(1 - Z(x)R(x) + C(x)Z(x)R(x))$. $K(x)$ is the veiling-free snowy image, $T(x)$ and $A(x)$ are the transmission map and atmospheric light. $C(x)$ and $Z(x)$ denote the chromatic aberration map for snow images and the snow mask, respectively. $J(x)$ is the snow-free image.

Earlier single image desnowing methods were based on the priors [6–11]. For instance, Pei *et al.* [6] utilized the image features prior of visibility and saturation to remove snowflakes. Recently,

¹Sixiang Chen, Tian Ye, Taodong Liao, JingXia Jiang, Erkang Chen and Peng Chen are with the School of Ocean Information Engineering, Jimei University, Xiamen, China. E-mail: {201921114013, 201921114031, 201921114028, 202021114006, ekchen, chenpeng}@jmu.edu.cn

²Yun Liu is with the College of Artificial Intelligence, Southwest University, Chongqing, China. yunliu@swu.edu.cn

³Erkang Chen and Peng Chen are with the Fujian Provincial Key Laboratory of Oceanic Information Perception and Intelligent Processing.

This research was supported by Natural Science Foundation of Fujian Province, China (2021J01867), Natural Science Foundation of Chongqing, China (cstc2020jcyj-msxmX0324), Xiamen Municipal Bureau of Ocean Development (22CZB013HJ04).

*: Corresponding author. †: Equal Contribution

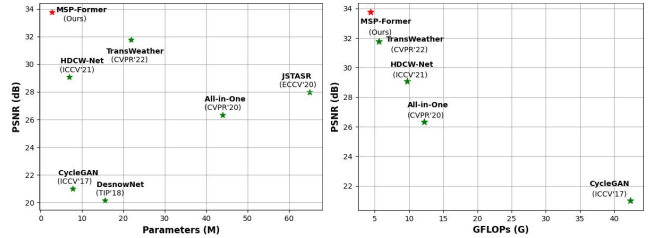


Fig. 1. Left. Trade-off between performance vs: number of parameters on CSD [15] testing dataset. Right. Trade-off between performance vs: computational cost calculated on 256×256 resolution.

with the development of CNNs, several desnowing networks [12–16] had been proposed to restore the clean image. JSTASR [14] employed a divide and conquer strategy to deal with the degradation of different sizes and haze veiling, respectively. In HDCW-Net [15], the dual-tree complex wavelet transform was applied to decompose the snow scene image. The hierarchical high and low frequency reconstruction network is used to remove the snow degradations and reconstruct the clean scene. DDMSNet [16] considered the semantic and depth information to precisely promote the network to tackle snow degradations.

Motivation. Despite that, two crucial points for effective desnowing are ignored: (i). *Targeted processing of multi-scale snow degradations and the relationship between them are the basis for handling complex snow scenes.* (ii). *Global context information is indispensable for the perfect reconstruction of clean scenes, which is overlooked in previous methods.* From Eq.1, the degraded snow scene usually contains the snowflake, snow streak, and veiling effect. Various degradations have different scale characteristics, making it easy to ignore some degradation information by fixing a single desnowing paradigm. In addition, the global snow scenes interaction cannot be acquired sufficiently via simple semantic and depth priors.

To settle above problems, we propose the MSP-Former, which particularly targets diverse snow degradations and global context information via a multi-scale self-attention paradigm. And the local snow degradation is also fully considered. Specifically, we construct a channel-dimensionally parallel network architecture, including a multi-scale projection (MSP) and a local capture module (LCB). MSP adopts the average pooling operation with different kernels and strides to aggregate diverse snow scenes and reduces the feature size. Furthermore, we separately project them into Key (\mathbf{K}) and Value (\mathbf{V}) for the multi-scale self-attention mechanism with global context information. Such a compact design leads our network to achieve SOTA performance at a much lower computational and pa-

parameter amount than previous ones, as shown in Fig.1.

More concretely, our contributions are summarized as follows:

- We propose an effective and lightweight single image snow removal architecture, MSP-Former, which is set as two parallel branches along the channel dimension. One target focuses on diverse snow degradations to support for the reconstruction of clean scenes and another branch aims to refine local details for snow scenes.
- Multi-scale Projection module primarily aggregates various snow degradations, which interacts with the global snow context information via multi-head self-attention to enhance the representation of reconstructing a clean image.
- We conduct extensive experiments to verify the superior performance of the proposed method. The experiments demonstrate that our network outperforms the previous state-of-the-art methods on multiple snow removal datasets, while the computational overhead and parameter amount are also significantly superior to previous methods.

2. METHOD

An overview of the MSP-Former architecture is shown in Fig.2, which is a multi-scale encoder and decoder architecture followed by UNet [17]. We employ 3×3 convolutional downsampling for each stage to reduce image size and increase dimension number. The features are split into two parts along the channel dimension and feed into our well-designed MSP and LCB modules for global clean scene reconstruction and local feature capture, respectively. We perform a channel shuffle operation before each channel concatenate, and ablation experiments prove that the channel shuffle operation can optimize our model. Afterward, we integrate the separately processed information along the channel dimension to improve the representability of our model on the image snow removal task. In the final stage, we add a refinement module based on the above design.

2.1. MSP Module

In snowy images, the ill-conditioned snow degradations of different scales overlaid on clean images make snow removal a challenging problem. To address this issue, we elaborate on a multi-scale projection (MSP) module to handle various degradations, which combines the global snow context information via self-attention.

2.1.1. MSP Self-Attention

For the vision transformer, as shown in Fig.3, given an input feature $X^{H \times W \times C}$, it is usually reshaped into a 3D sequence $X_s^{N \times C}$ and a linear layer is employed to project X into Query(**Q**), Key(**K**), Value(**V**), can be expressed in the following form:

$$\text{Projection : } \mathbf{Q} = W_q X_s, \mathbf{K} = W_k X_s, \mathbf{V} = W_v X_s, \quad (2)$$

where W_q, W_k, W_v are linear projection parameters. Nevertheless, due to fixed patch embedding, separate projections result in a fixed receptive field for each sequence in the global modeling after linear layer transformation. This is very disadvantageous for recovering variable degradation information in complex snow images.

To solve this problem, in MSP self-attention, we first use a multi-scale avgpool to aggregate different information, fully capturing diverse scale snow information and providing multi-head self-attention with a richer snow degradation representation capability. At the same time, based on the above operations, we reduce the image

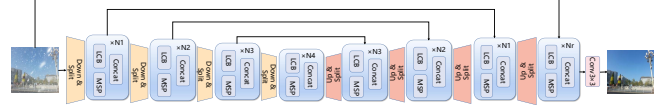


Fig. 2. Our MSP-Former consists of an encoder-decoder, and there is a skip connection between the corresponding stages inspired by UNet [17]. Ultimately, we use a 3×3 convolution to transform the output image.

size required for K and V projection to reduce the amount of self-attention computation, and we can express the aggregated features as:

$$X_1^{\frac{H}{R_1} \times \frac{W}{R_1} \times C} = \text{Avgpool}_{K_1}^{S=R_1}(X^{H \times W \times C}), \quad (3)$$

$$X_2^{\frac{H}{R_2} \times \frac{W}{R_2} \times C} = \text{Avgpool}_{K_2}^{S=R_2}(X^{H \times W \times C}), \quad (4)$$

among them, X_1 and X_2 are different feature maps, and K and S represent pooled kernel and stride. Then we use a linear layer to re-project the features that aggregate different local information to Key(**K**) and Value(**V**), respectively, for Scaled Dot-product Attention with the original Query(**Q**) to improve the multi-scale representation ability of self-attention. Such a paradigm incorporates global context information and multi-scale degraded snow scenes into the design category, which carefully considers the critical motivation for snow removal. Inspired by multi-head self-attention [18], we perform multi-head self-attention (MSA) separately for Key(**K**) and Value(**V**) with different degradations, and finally concat them together. The formula of the multi-scale projection can be expressed as follows:

$$K_{\{1,2\}} = W_{k\{1,2\}} X_{\{1,2\}}, V_{\{1,2\}} = W_{v\{1,2\}} X_{\{1,2\}}, \quad (5)$$

$$\text{MSA}(X) = \text{Concat}\left(\text{Softmax}\left(\frac{\mathbf{Q}_h \mathbf{K}_{h\{1,2\}}^\top}{\sqrt{D_h}}\right) \mathbf{V}_{h\{1,2\}}\right), \quad (6)$$

where h represents multi-head processing, and D_h is the dimension of each head. Considering the fine information and low-level details required in the process of self-attention, we add a depth-wise convolution before the point product of Value(**V**) to improve the local retention ability like [19] does.

2.1.2. MSP Transformer Block

Like the vanilla Transformer, the MSP transformer block consists of two critical constructions, MSP Self-Attention and ConvFFN. It adds Layernorm before each part while adding residual connections to the MSP Self-Attention and ConvFFN parts to stabilize the training network. The following formula can describe the entire block:

$$\begin{aligned} X' &= X + \text{MSP-Self-Attention}(\text{LN}(X)), \\ Y &= X' + \text{ConvFFN}(\text{LN}(X')), \end{aligned} \quad (7)$$

We continue to use ConvFFN [20], which has been demonstrated to possess more potential to replace the traditional MLP feedforward network to alleviate its shortcomings in local modeling, similar to the PVT [20] approach.

2.2. LCB Module

In the single snow removal task, both the global degradation and the local degradation consisting of snow patches are included, so

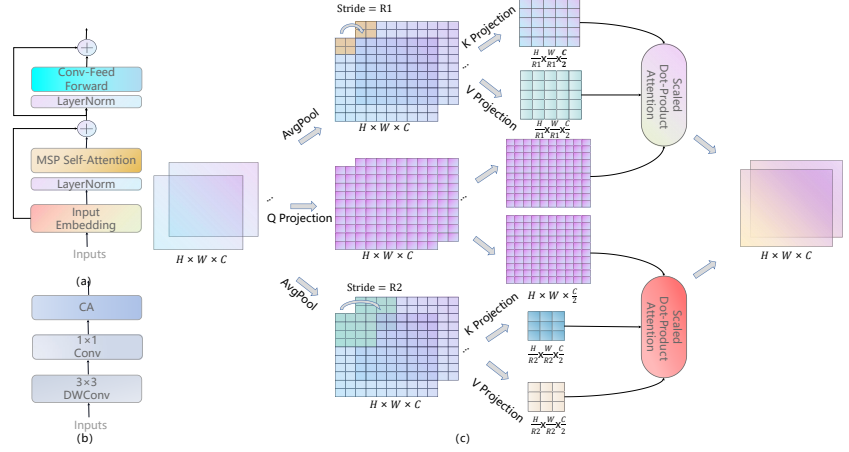


Fig. 3. (a) is the multi-scale projection(MSP) module, (b) is the local capture block(LCB) module, and (c) is the multi-scale projection self-attention mechanism(MSP Self-Attention) in the MSP module.

the local context information determines the detailed features of the restored image. Unlike the multi-scale self-attention module introduced above, we develop a local capture module parallel to the MSP module. It is worth mentioning that it differs from the complex calculation required by the transformer module. It only requires minimal computation and parameters, which plays a crucial role in the model’s performance-parameters trade-off in the snow removal task.

As illustrated in Fig.2(b), for the input $X^{H \times W \times C}$, we utilize 3×3 depth-wise convolution to excavate local snow features and exploit a 1×1 convolution for inter-channel interactions. In addition, the transformer is essentially self-modeling at the spatial level between patches. It lacks the modeling between channels, so we add channel attention [21] to the local capture module to increase the overall representation ability of the model. We can compute the whole LCB module as follows:

$$LCB(X^{H \times W \times C}) = CA(\text{Conv}_{K=1}(\text{DWConv}_{K=3}(X))), \quad (8)$$

where K is the convolution kernel and CA is the channel attention.

2.3. Loss Function

We introduce the Charbonnier Loss [22] as our reconstruction loss:

$$\mathcal{L}_{rec} = \mathcal{L}_{\mathcal{CR}}(\mathcal{M}(X) - \mathcal{J}_{gt}), \quad (9)$$

where the \mathcal{M} is proposed network, X and \mathcal{J}_{gt} stand for input and ground-truth. $\mathcal{L}_{\mathcal{CR}}$ denotes the Charbonnier loss, which can be express as:

$$\mathcal{L}_{\mathcal{CR}} = \frac{1}{N} \sum_{i=1}^N \sqrt{\|X^i - Y^i\|^2 + \epsilon^2}, \quad (10)$$

where constant ϵ empirically set to $1e^{-3}$ for all experiments.

3. EXPERIMENTS

Implementation Details. In the training details of the proposed MSP-Former, we use AdamW optimizer with the first and second momentum terms of (0.9, 0.999), the weight decay is $5e^{-4}$ to train our framework. We set the initial learning rate to 0.0007 and employ linear decay after 250 epochs. For data augmentation, we adopt horizontal flip and random rotation by 90, 180, 270 degrees. We randomly crop a 256×256 patch as input to train 600 epochs. For

Table 1. Desnowing results on the CSD [15], SRRS [14] and Snow 100K [12] datasets (PSNR(dB)/SSIM). Bold and underline indicate the best and second metrics.

Method	CSD (2000) [15]		SRRS (2000) [14]		Snow 100K (2000) [12]		#Param	#GMacs
	PSNR ↑	SSIM ↑	PSNR ↑	SSIM ↑	PSNR ↑	SSIM ↑		
(TIP’18)DesnowNet [12]	20.13	0.81	20.38	0.84	30.50	0.94	15.6M	1.7KG
(CVPR’18)CycleGAN [23]	20.98	0.80	20.21	0.74	26.81	0.89	7.84M	42.38G
(CVPR’20)All in One [13]	26.31	0.87	24.98	0.88	26.07	0.88	44M	12.26G
(ECCV’20)STASR [14]	27.96	0.88	25.82	0.89	23.12	0.86	65M	—
(ICCV’21)HDCW-Net [15]	29.06	0.91	27.78	0.92	31.54	<u>0.95</u>	6.99M	9.78G
(CVPR’22)TransWeather [24]	<u>31.76</u>	<u>0.93</u>	<u>28.29</u>	<u>0.92</u>	<u>31.82</u>	0.93	21.9M	5.64G
MSP-Former	33.75	0.96	30.76	0.95	33.43	0.96	2.83M	4.42G

a concise description, we illustrate our MSP-Former framework design. At each stage of the network, we set the channel dimensions to $\{32, 64, 128, 256\}$ respectively, and we gradually increase the number of MSP and LCB modules to N_1, N_2, N_3, N_4 , which are set to 2, 3, 4, and 6 in our network. We specify the strides R_1 and R_2 of each layer’s multi-scale average pooling as $R_1 = \{16, 8, 4, 2\}$ and $R_2 = \{8, 4, 2, 1\}$, the pooling kernel is also set as $K_1 = \{16, 8, 4, 2\}$, $K_2 = \{8, 4, 2, 1\}$. At the shallowest layer of the decoder, we also add an MSP and an LCB module to refine the original resolution image to improve the final output, in which N_r, K_1, R_1 and K_2, R_2 are set to 1, 16, 16, 8, 8.

Quantitative Analysis. In this section, we compare the performance of our method with other existing snow removal methods: [12], [23], [13], [14], [15] and [24] on three benchmarks [12, 14, 15]. To ensure fairness, for the methods without snow datasets training, we re-train to meet the latest evaluation criteria of the previous snow removal [15] and take the best training results for comparison. Table 1 reports the results on different snow datasets, which shows that our model outperforms all SOTA desnowing methods. On Snow100K [12], SRRS [14] and CSD [15] testing sets, MSP-Former achieves 1.99 dB, 2.47 dB and 1.61 dB improvement on PSNR metric, and is also significantly ahead of the most advanced methods on SSIM.

Parameters and Computational Complexity Analysis. For an excellent model, parameters and computation are also within the scope of measurement. The number of parameters determines whether the model is lightweight, and the amount of calculation measures the model’s efficiency. We present the comparison results of compu-



Fig. 4. Visual comparison of our method (MSP-Former) and the SOTA methods on the synthetic dataset CSD [15].

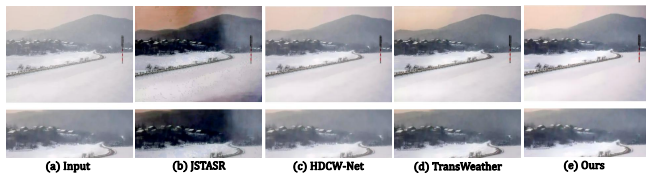


Fig. 5. Visual comparison of desnowing on the real-world snow image.

tation of 256×256 size and parameters with state-of-the-art snow removal method in Table 1. We notice that our MSP-Former is better than the previous SOTA approaches in terms of both parameters and the amount of calculation, which is only 2.83M and 4.26GMacs. We outperform HDCW-Net [15] and TransWeather [24] in terms of performance-parameter trade-off.

Visual Comparison. We compare the visual performance of MSP-Former and other state-of-the-art methods for snow removal on desnowing datasets and real snow image, which are presented in Fig.4 and 5. It can be seen that the previous desnowing methods are not able to completely remove all snow scenes at one time due to ignored context information, especially small snow spots and snow marks. Instead, MSP-Former can remove snow degradation of various sizes very well, superior to previous SOTA methods in detail and background restoration. In particular, our method also attracts certain advantages in the recovery of fine snow points and overall color regions.

3.1. Ablation Study

For the ablation study, we employ the Charbonnier loss [22] as our loss function and train on the CSD [15] dataset with 256×256 for 200 epochs to test the effectiveness of our model.

Effectiveness of MSP-Self Attention. To verify the effect of our avgpool local aggregate projection self-attention(AA), we replace our scheme with spatial-reduction attention(SRA) proposed by PVT [20] and max-pooling aggregate projection(MA). The results are shown in Table 2. Experiments demonstrate avgpooling attracts the best performance in targeting various snow degradations. In addition, We also conduct multi-scale projection(MSP) and single-scale projection(SSP) ablation experiments to verify that our MSP Self-Attention can achieve non-trivial effects on snow removal due to its adaptation to various scales of snow degradation information.

Table 2. Ablation Study on the MSP-Self Attention.

Model	#Param	#GFlops	PSNR	SSIM
SRA	3.28M	4.61G	29.84	0.931
MA	2.83M	4.42G	28.57	0.903
SSP	2.83M	4.39G	29.49	0.921
MSP(Ours)	2.83M	4.42G	<u>30.12</u>	<u>0.935</u>

Effectiveness of LCB Module. We verify the effect of our LCB module in ablation experiments. We designed three schemes to conduct our experiments. As described in Table 3, we observe that parallel LCB modules can boost the model’s overall recovery performance, which indicates that the model can simultaneously focus on global scene reconstruction and fine-grained recovery of local details. It is worth describing that we found adding channel attention to the convolution module can play a vital role in the overall representative ability of the architecture with only a small amount of parameters and computation.

Table 3. Ablation Study on the LCB Module and channel shuffle.

Model	#Param	#GFlops	PSNR	SSIM
w/o LCB	2.60M	4.26G	29.21	0.919
LCB w/o CA	2.76M	4.42G	29.61	0.923
w/o CS	2.83M	4.26G	29.46	0.923
LCB(Ours)	2.83M	4.26G	<u>30.12</u>	<u>0.935</u>

Effectiveness of Channel Shuffle. We remove and add channel shuffle(CS) operations respectively to observe the changes in model performance, which are described in Table 3. The experiment demonstrates that the information reorganization between channels brought by the channel shuffle operations can improve the effects of the network.

4. CONCLUSION

This paper proposes a single-image snow removal method with a multi-scale projection transformer. Specifically, we employ multi-scale projections to target diverse degradations and combine global context information to promote the reconstruction of the clean scene via multi-head self-attention. On the other hand, we exploit our designed lightweight local capture module for local feature mining. The clever parallel combination of the two can achieve state-of-the-art performance on the snow removal task with a meager amount of parameters and computation, achieving a performance-parameters trade-off.

5. REFERENCES

- [1] Tian Ye, Yunchen Zhang, Mingchao Jiang, Liang Chen, Yun Liu, Sixiang Chen, and Erkang Chen, "Perceiving and modeling density for image dehazing," in *Computer Vision–ECCV 2022: 17th European Conference, Tel Aviv, Israel, October 23–27, 2022, Proceedings, Part XIX*. Springer, 2022, pp. 130–145.
- [2] Tian Ye, Sixiang Chen, Yun Liu, Yi Ye, Erkang Chen, and Yuche Li, "Underwater light field retention: Neural rendering for underwater imaging," in *Proceedings of the IEEE/CVF Conference on Computer Vision and Pattern Recognition (CVPR) Workshops*, June 2022, pp. 488–497.
- [3] Yeying Jin, Wenhan Yang, and Robby T Tan, "Unsupervised night image enhancement: When layer decomposition meets light-effects suppression," in *Computer Vision–ECCV 2022: 17th European Conference, Tel Aviv, Israel, October 23–27, 2022, Proceedings, Part XXXVII*. Springer, 2022, pp. 404–421.
- [4] Syed Waqas Zamir, Aditya Arora, Salman Khan, Munawar Hayat, Fahad Shahbaz Khan, and Ming-Hsuan Yang, "Restormer: Efficient transformer for high-resolution image restoration," *arXiv preprint arXiv:2111.09881*, 2021.
- [5] Tian Ye, Yun Liu, Yunchen Zhang, Sixiang Chen, and Erkang Chen, "Mutual learning for domain adaptation: Self-distillation image dehazing network with sample-cycle," *arXiv preprint arXiv:2203.09430*, 2022.
- [6] Soo-Chang Pei, Yu-Tai Tsai, and Chen-Yu Lee, "Removing rain and snow in a single image using saturation and visibility features," in *2014 IEEE International Conference on Multimedia and Expo Workshops (ICMEW)*. IEEE, 2014, pp. 1–6.
- [7] Yinglong Wang, Shuaicheng Liu, Chen Chen, and Bing Zeng, "A hierarchical approach for rain or snow removing in a single color image," *IEEE Transactions on Image Processing*, vol. 26, no. 8, pp. 3936–3950, 2017.
- [8] Dhanashree Rajderkar and PS Mohod, "Removing snow from an image via image decomposition," in *2013 IEEE International Conference ON Emerging Trends in Computing, Communication and Nanotechnology (ICECCN)*. IEEE, 2013, pp. 576–579.
- [9] Xianhui Zheng, Yinghao Liao, Wei Guo, Xueyang Fu, and Xinghao Ding, "Single-image-based rain and snow removal using multi-guided filter," in *International conference on neural information processing*. Springer, 2013, pp. 258–265.
- [10] Tian Ye, Sixiang Chen, Yun Liu, Yi Ye, Jinbin Bai, and Erkang Chen, "Towards real-time high-definition image snow removal: Efficient pyramid network with asymmetrical encoder-decoder architecture," in *Proceedings of the Asian Conference on Computer Vision (ACCV)*, December 2022, pp. 366–381.
- [11] Sixiang Chen, Tian Ye, Yun Liu, Erkang Chen, Jun Shi, and Jingchun Zhou, "Snowformer: Scale-aware transformer via context interaction for single image desnowing," *arXiv preprint arXiv:2208.09703*, 2022.
- [12] Yun-Fu Liu, Da-Wei Jaw, Shih-Chia Huang, and Jenq-Neng Hwang, "Desnownet: Context-aware deep network for snow removal," *IEEE Transactions on Image Processing*, vol. 27, no. 6, pp. 3064–3073, 2018.
- [13] Ruoteng Li, Robby T Tan, and Loong-Fah Cheong, "All in one bad weather removal using architectural search," in *Proceedings of the IEEE/CVF Conference on Computer Vision and Pattern Recognition*, 2020, pp. 3175–3185.
- [14] Wei-Ting Chen, Hao-Yu Fang, Jian-Jiun Ding, Cheng-Che Tsai, and Sy-Yen Kuo, "Jstasr: Joint size and transparency-aware snow removal algorithm based on modified partial convolution and veiling effect removal," in *European Conference on Computer Vision*. Springer, 2020, pp. 754–770.
- [15] Wei-Ting Chen, Hao-Yu Fang, Cheng-Lin Hsieh, Cheng-Che Tsai, I Chen, Jian-Jiun Ding, Sy-Yen Kuo, et al., "All snow removed: Single image desnowing algorithm using hierarchical dual-tree complex wavelet representation and contradict channel loss," in *Proceedings of the IEEE/CVF International Conference on Computer Vision*, 2021, pp. 4196–4205.
- [16] Kaihao Zhang, Rongqing Li, Yanjiang Yu, Wenhan Luo, and Changsheng Li, "Deep dense multi-scale network for snow removal using semantic and depth priors," *IEEE Transactions on Image Processing*, vol. 30, pp. 7419–7431, 2021.
- [17] Olaf Ronneberger, Philipp Fischer, and Thomas Brox, "U-net: Convolutional networks for biomedical image segmentation," in *International Conference on Medical image computing and computer-assisted intervention*. Springer, 2015, pp. 234–241.
- [18] Alexey Dosovitskiy, Lucas Beyer, Alexander Kolesnikov, Dirk Weissenborn, Xiaohua Zhai, Thomas Unterthiner, Mostafa Dehghani, Matthias Minderer, Georg Heigold, Sylvain Gelly, et al., "An image is worth 16x16 words: Transformers for image recognition at scale," *arXiv preprint arXiv:2010.11929*, 2020.
- [19] Sucheng Ren, Daquan Zhou, Shengfeng He, Jiashi Feng, and Xinchao Wang, "Shunted self-attention via multi-scale token aggregation," in *Proceedings of the IEEE/CVF Conference on Computer Vision and Pattern Recognition*, 2022, pp. 10853–10862.
- [20] Wenhai Wang, Enze Xie, Xiang Li, Deng-Ping Fan, Kaitao Song, Ding Liang, Tong Lu, Ping Luo, and Ling Shao, "Pyramid vision transformer: A versatile backbone for dense prediction without convolutions," in *Proceedings of the IEEE/CVF International Conference on Computer Vision*, 2021, pp. 568–578.
- [21] Jie Hu, Li Shen, and Gang Sun, "Squeeze-and-excitation networks," in *Proceedings of the IEEE conference on computer vision and pattern recognition*, 2018, pp. 7132–7141.
- [22] Pierre Charbonnier, Laure Blanc-Feraud, Gilles Aubert, and Michel Barlaud, "Two deterministic half-quadratic regularization algorithms for computed imaging," in *Proceedings of 1st International Conference on Image Processing*. IEEE, 1994, vol. 2, pp. 168–172.
- [23] Deniz Engin, Anil Genç, and Hazim Kemal Ekenel, "Cycle-dehaze: Enhanced cyclegan for single image dehazing," in *Proceedings of the IEEE conference on computer vision and pattern recognition workshops*, 2018, pp. 825–833.
- [24] Jeya Maria Jose Valanarasu, Rajeev Yasarla, and Vishal M Patel, "Transweather: Transformer-based restoration of images degraded by adverse weather conditions," in *Proceedings of the IEEE/CVF Conference on Computer Vision and Pattern Recognition*, 2022, pp. 2353–2363.